Yliniemi, Kirsi; Nguyen, Nhat Truong; Mohajernia, Shiva; Liu, Ning; Wilson, Benjamin; Schmuki, Patrik; Lundström, Mari

A direct synthesis of platinum/nickel co-catalysts on titanium dioxide nanotube surface from hydrometallurgical-type process streams

Published in:
Journal of Cleaner Production

DOI:
10.1016/j.jclepro.2018.08.022

Published: 10/11/2018

Document Version
Publisher's PDF, also known as Version of record

Journal of Cleaner Production 201 (2018) 39–48

Contents lists available at ScienceDirect

Journal of Cleaner Production

journal homepage: www.elsevier.com/locate/jclepro

A direct synthesis of platinum/nickel co-catalysts on titanium dioxide nanotube surface from hydrometallurgical-type process streams

Kirsi Yliniemi [a], Nhat Truong Nguyen [b], Shiva Mohajernia [b], Ning Liu [b], Benjamin P. Wilson [a], Patrik Schmuki [b, c], Mari Lundström [a, *]

[a] School of Chemical Engineering, Aalto University, P.O. Box. 16200, 00076, Aalto, Finland
[b] Friedrich-Alexander University of Erlangen-Nuremberg, Department of Materials Science, Institute for Surface Science and Corrosion (LKO), Martensstraße 7, 91058 Erlangen, Germany
[c] Department of Chemistry, King Abdulaziz University, 80203 Jeddah, Saudi Arabia

ARTICLE INFO

Article history:
Received 3 January 2018
Received in revised form
8 June 2018
Accepted 2 August 2018
Available online 4 August 2018

Keywords:
Electrodeposition
Redox replacement
Hydrogen evolution
Photocatalysis
Circular economy
Sustainable nanoparticles

ABSTRACT

Solutions that simulate hydrometallurgical base metal process streams with high nickel (Ni) and minor platinum (Pt) concentrations were used to create Pt/Ni nanoparticles on TiO_2 nanotube surfaces. For this, electrochemical deposition – redox replacement (EDRR) was used that also allowed to control the nanoparticle size, density and Pt/Ni content of the deposited nanoparticles. The Pt/Ni nanoparticle decorated titanium dioxide nanotubes (TiO_2 nanotubes) become strongly activated for photocatalytic hydrogen (H_2) evolution. Moreover, EDRR facilitates nanoparticle formation without the need for any additional chemicals and is more effective than electrodeposition alone. Actually, a 10,000-time enrichment level of Pt took place on the TiO_2 surface when compared to Pt content in the solution with the EDRR method. The results show that hydrometallurgical streams offer great potential as an alternative raw material source for industrial catalyst production when coupled with redox replacement electrochemistry.

1. Introduction

This paper outlines a viable method to grow Pt/Ni nanoparticles on TiO_2 nanotube surfaces, directly from solutions that resemble those available in industrial nickel processing. Global nickel resources originate from two different types of ores, sulfides and laterites, which in hydrometallurgical Ni recovery are dissolved to either chloride, sulfate or ammonia media, with or without pyrometallurgical pre-treatment steps. Ni recovery from these solutions is typically achieved by solvent extraction-electrowinning (i.e. a pure electrodeposition) route, although hydrogen reduction and different chemical precipitation methods may also be used. As a result, all Ni processing produces hydrometallurgical solutions that not only contain nickel but also a variety of other metals originally present in the ore - like cobalt, copper and precious metals - and the processes are usually optimised also to recover these other metals (Crundwell et al., 2011). In spite of this, such solutions can still contain trace amounts of precious metals, which are not recovered from solutions due to a high concentration ratio between the base metal (such as Ni) and trace metals (such as Pt).

This is of particular importance in view of the global scarcity of metal resources that has become an imminent concern (Peck et al., 2015) and thus, improved recycling and recovering of metals from impure process solutions, acidic industrial side-streams and other waste streams is becoming a necessity. At the same time, emerging technologies like fuel cells may increase the demand for Pt as a catalyst material even further (Peck et al., 2015) and therefore, identification of alternative (secondary) raw material sources for platinum group metal (PGM) based catalysts is essential.

Ni-Pt combinations have been proved to be extremely effective catalyst materials (Debe, 2012; He et al., 2011, 2013; Kühl and Strasser, 2016; Shao et al., 2016) and thus, process and side-streams associated with Ni metal (McDonald and Whittington, 2008a,b) could be potential raw material sources when trace amounts of Pt is present, especially as annual global nickel production is over 2000 Gg (i.e. 2 million tonnes) and expected to increase up to 140–175% by 2025 (Elshkaki et al., 2017). However, due to the high concentration ratio between Ni and precious metals, the hydrometallurgical solutions in nickel production have not been

* Corresponding author.
E-mail address: mari.lundstrom@aalto.fi (M. Lundström).

https://doi.org/10.1016/j.jclepro.2018.08.022

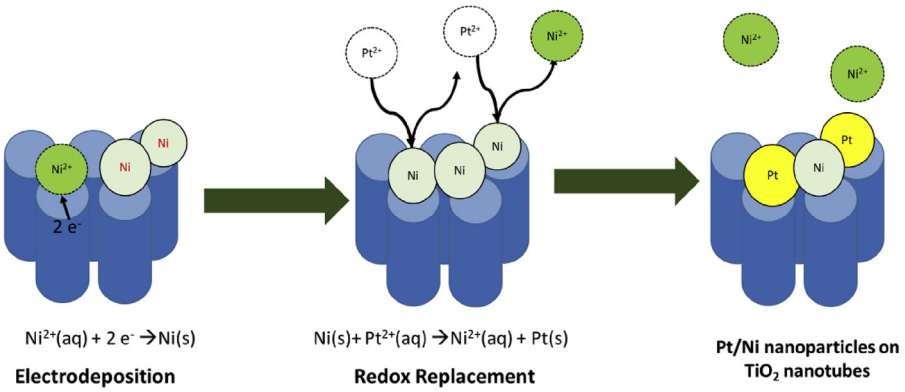

Fig. 1. Schematic of the electrodeposition – redox replacement (EDRR) process from a solution containing Ni and Pt showing the formation of Pt/Ni nanoparticles on the TiO_2 nanotubes.

considered suitable for recovery of precious metals, and even less, for production of a high-added value Pt catalyst.

On the other hand, the toxic nature of nickel solutions – which are inevitable in hydrometallurgy in order to fulfil the ever increasing global nickel demand –would require new methodologies of how to fully exploit these solutions and also, the minor components present in them. The results presented here show that utilising redox replacement reactions the formation of Pt/Ni catalysts from such solutions is indeed possible, without any additional chemicals.

Usually the redox replacement reaction is used in conjunction with electrochemical deposition and this is the case in our studies (Fig. 1). Firstly, Ni is electrodeposited and then, the redox replacement reaction takes place spontaneously between electrodeposited Ni and Pt^{2+} ions due to the difference in the reduction potentials: the deposited Ni is oxidised by Pt^{2+} and dissolved back to solution as Ni^{2+}, whilst Pt^{2+} is reduced to Pt and deposited on the electrode. The half-reaction for the oxidation of Ni is shown in Reaction 1a and the reduction of Pt^{2+} in Reaction 1b, together with their respective standard electrode potentials (E° vs. SHE).

$$Ni_s \rightarrow Ni_{aq}^{2+} + 2e^- \quad E^{\circ}(\text{ox}) = +0.25\ \text{V vs. SHE} \tag{1a}$$

$$Pt_{aq}^{2+} + 2e^- \rightarrow Pt_s \quad E^{\circ}(\text{red}) = +1.20\ \text{V vs. SHE} \tag{1b}$$

The overall redox reaction is displayed in Reaction 2, together with the standard reaction potential, which is the driving force for the spontaneous redox replacement reaction:

$$Ni_s + Pt_{aq}^{2+} \rightarrow Ni_{aq}^{2+} + Pt_s \quad E^{\circ}(\text{RR}) = +1.45\ \text{V vs. SHE} \tag{2}$$

In contrast to other electrochemical-redox replacement methods like electrochemical-atomic layer deposition (e-ALD) (Gregory and Stickney, 1991; Vaidyanathan et al., 2006) or surface-limited redox replacement (SLRR) (Brankovic et al., 2001), the goal here is not to deposit smooth monolayers but utilise electrodeposition-redox replacement method (EDRR) to create functional Pt/Ni catalysts directly from solutions resembling hydrometallurgical Ni process solutions.

Moreover, this one step approach differs from those presented in literature about Pt/Ni surfaces prepared by EDRR (Papadimitriou et al., 2008, 2010; Rettew et al., 2009; Tegou et al., 2010; Wang et al., 2011; Zhang et al., 2012) or electroless deposition-redox replacement (Tamašauskaitė-Tamašiūnaitė et al., 2013, 2014). In these previous studies, all the solutions have been optimised for the application, i.e. Pt and Ni concentrations of synthetic solutions are tailored for the most effective catalyst formation and they do not represent industrial solutions. Conversely, this paper demonstrates – for the very first time – that non-optimised solutions and side-streams could be a potential raw material sources for functional Pt/Ni catalyst surfaces. These solutions are indeed challenging as in hydrometallurgical Ni process solutions the Ni content is high and

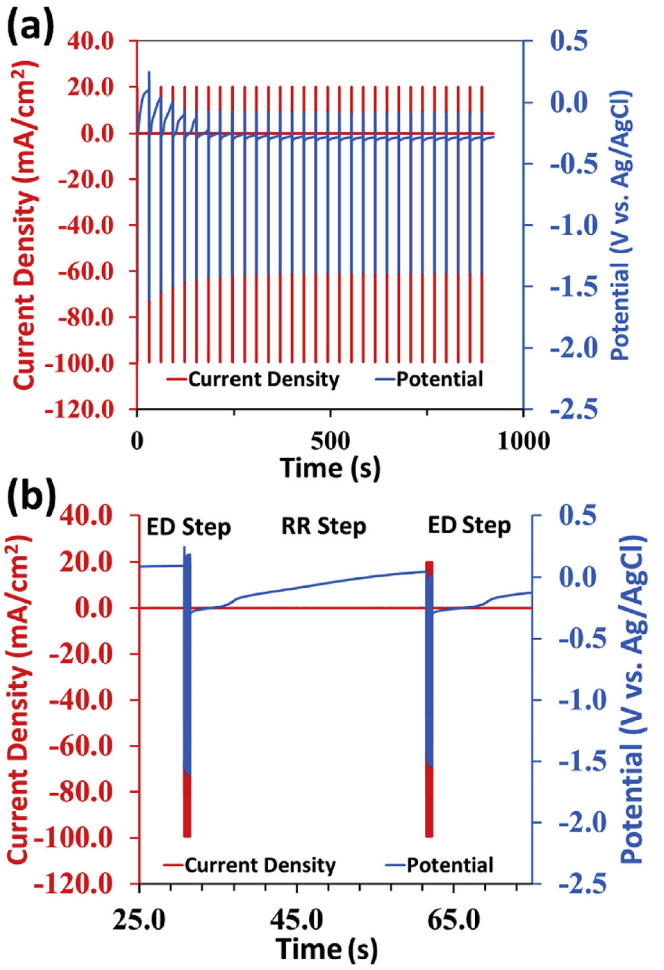

Fig. 2. An example of electrodeposition – redox replacement curves on flat TiO_2 surface. Solution: 100 ppm Pt, 60 g/l Ni and 10 g/l H_2SO_4, EDRR parameters: i(cathodic) = −100 mA/cm^2 for 10 ms, i(anodic) = 20 mA/cm^2 for 10 ms, total number of pulses: 74 (37 cathodic-anodic pulse pairs), redox replacement time: 30 s and number of EDRR cycles: 30. (a) Full EDRR data, (b) magnification in 25–75 s.

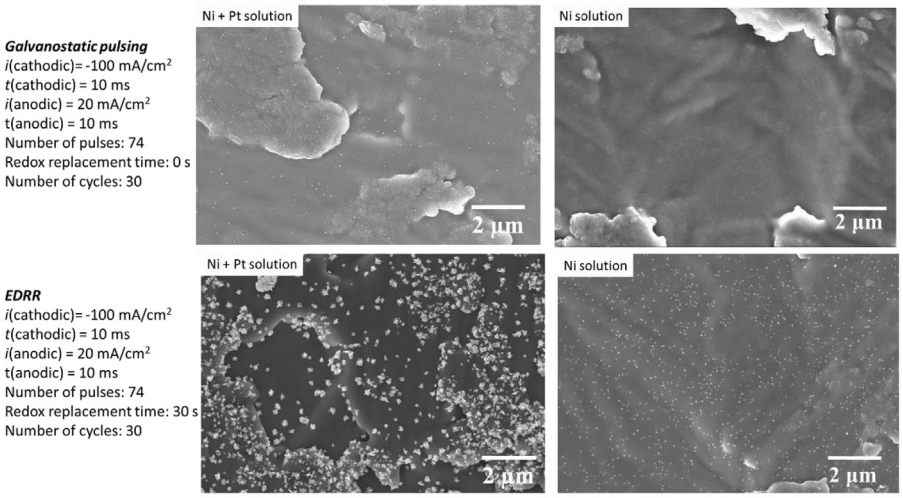

Fig. 3. Comparison of deposited nanoparticles on flat TiO_2 when using pure galvanostatic pulsing or EDRR method, from solution containing 100 ppm Pt, 60 g/l Ni and 10 g/l H_2SO_4 (Ni + Pt solution) or 60 g/l Ni and 10 g/l H_2SO_4 (Ni solution).

Pt content extremely low: for a 10 ppm Pt solution, Ni/Pt concentration ratio is typically ≈ 20,000.

Earlier, the authors have demonstrated that Ag can be recovered from Zn based hydrometallurgical solutions by EDRR (Halli et al., 2017) and Au from copper based solutions (Korolev et al., 2018) whereas this current paper goes beyond that approach: instead of pure recovery of a precious metal, functional Pt/Ni catalytic surfaces are produced and used without any further modifications for photocatalytic H_2 generation.

From an industrial perspective, the possibility to utilise under sourced side-streams and process solutions for catalyst production makes EDRR already very attractive method but it has also further advantages: EDRR does not demand any additional chemicals, unlike cementation (precipitation) or solvent extraction traditionally used in hydrometallurgy for metal recovery, no neutralization chemicals are needed either, and when compared to electrowinning (pure electrodeposition), EDRR is more effective with solutions of trace amount of precious metals. This all makes the EDRR method more sustainable than the competing methods.

Overall, this research demonstrates a new route for the exploitation underutilised industrial side-stream solutions, which not only leads to the formation of catalytic surfaces for clean energy production but also has the added benefit of reducing/eliminating the presence of potentially toxic material (Pt) from industrial Ni processing. Furthermore, this method provides a platform for the cost and material competitive large-scale catalyst production based on the principles of circular economy.

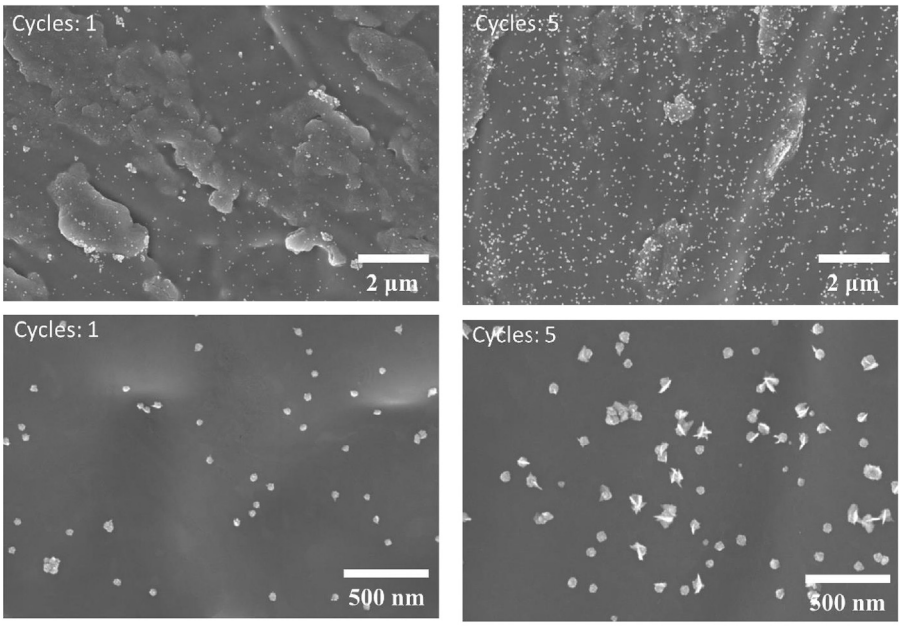

Fig. 4. Effect of the first EDRR cycles on Pt/Ni nanoparticle nucleation from 100 ppm Pt, 60 g/l Ni and 10 g/l H_2SO_4 solution: SEM images after the first and the fifth cycle with 10,000 magnification (upper row) and 50,000 magnification (lower row). EDRR parameters: i(cathodic) = −100 mA/cm^2 for 10 ms, i(anodic) = 20 mA/cm^2 for 10 ms, total number of pulses: 74 (37 cathodic-anodic pulse pairs), redox replacement time: 30 s.

2. Materials and methods

Flat TiO_2 surfaces were prepared by anodising Ti foil (99.9%) at 20 V for 15 min in 0.5 M H_2SO_4. In contrast, TiO_2 nanotubes were prepared by the immersion of Ti foil in a tri-ethylene glycol electrolyte consisting of 0.3 M NH_4F and 3 M H_2O, at 60 V at 60 °C for 15 min. After anodising, all the samples were annealed in air at 450 °C for 1 h.

Ni nanoparticles were prepared on TiO_2 surfaces by the electrodeposition – redox replacement (EDRR) method (Ivium CompactStat) from a solution containing 60 g/l nickel (from $NiSO_4 \cdot 6H_2O$, ACS grade, Sigma-Aldrich) and 10 g/l H_2SO_4 (95–98%, p.a., Carl Roth), while Pt/Ni nanoparticles were deposited from the same base solution (60 g/l nickel + 10 g/l H_2SO_4) having 10 ppm or 100 ppm Pt (from 1000 mg/l AAS standard, Sigma-Aldrich). Either flat TiO_2 or TiO_2 nanotube surfaces – with a geometric area 0.5 cm^2 - were used as the working electrode, with a Pt sheet (6 cm^2) as the counter electrode and Ag/AgCl in 3 M KCl as the reference electrode. The distance between working and counter electrode was 2 cm and the volume of the solution was 20–25 ml.

In EDRR method, the electrodeposition step (ED step) was performed galvanostatically and consisted of a total 74 short cathodic and anodic current pulses. After 37 cathodic-anodic pulse pairs, a redox replacement (RR) step was performed. During this step, no external current or voltage was applied but open circuit potential (OCP) was recorded until a pre-determined time had elapsed. After this, the EDRR cycle was repeated - first with 37 cathodic-anodic pulse pairs followed by a RR step.

In the case of the flat TiO_2 surfaces, the cathodic and anodic current pulses had a duration of 10 ms each and the current density was −100 mA/cm^2 and +20 mA/cm^2, respectively. The RR step time was either 10, 30 or 60 s and the number of full EDRR cycles was varied (10, 20 or 30 cycles). For TiO_2 nanotube surfaces the conditions were modified, such that the cathodic pulse durations were 4 s at −30 mA/cm^2 and anodic pulses 10 ms at +30 mA/cm^2, to reflect the higher surface area and lower conductivity of the tubes. The associated RR time was set to be between 60 and 240 s and the number of cycles was either 10 or 20 cycles.

Field-emission scanning electron microscope (FE-SEM Hitachi S4800) was used to characterize the morphology of the samples, whereas X-ray photoelectron spectroscopy (XPS, PHI 5600) provided the chemical composition of the samples. In XPS, the signal intensity was divided by a relative sensitivity factor (RSF) and normalized over all of the elements detected. All data processing was performed using MultiPack v.9.6.0 software.

Photocatalytic H_2 generation measurements were conducted by irradiating the TiO_2 samples with an AM 1.5 solar simulator (100 mW/cm^2) in a quartz tube containing a 20 vol% ethanol-water solution for 5 h. The amount of produced H_2 was measured by using a gas chromatograph (GCMS-QO2010SE, Shimadzu) equipped with a thermal conductivity detector and a Restek micropacked Shin Carbon ST column (2 m × 0.53 mm). The quartz reactor was purged with N_2 gas for 10 min to remove O_2 prior to the initiation of the photocatalytic experiments.

3. Results and discussion

Pt/Ni nanoparticles are formed on TiO_2 surface during electrodeposition-redox replacement (EDRR) cycling and a typical EDRR measurement is shown in Fig. 2: short cathodic + anodic current pulses (during the ED step) are followed by redox replacement (RR step) and the EDRR procedure is cycled a number of times. The EDRR profiles for all samples are shown in Supporting Information (Fig. S1).

The ED step (electrodeposition) consists of galvanostatic pulsing between cathodic and anodic currents. Firstly, Ni and possibly some Pt is deposited during the short cathodic current pulse, though simultaneous H_2 evolution - that disturbs the deposition - may also take place. This is overcome by applying a short anodic current pulse that not only results in hydrogen desorption, but also makes more surface sites available for deposition in the following cathodic pulse (Kollia et al., 1990; Spanou and Pavlatou, 2010). During the RR step (redox replacement) there is a spontaneous replacement of

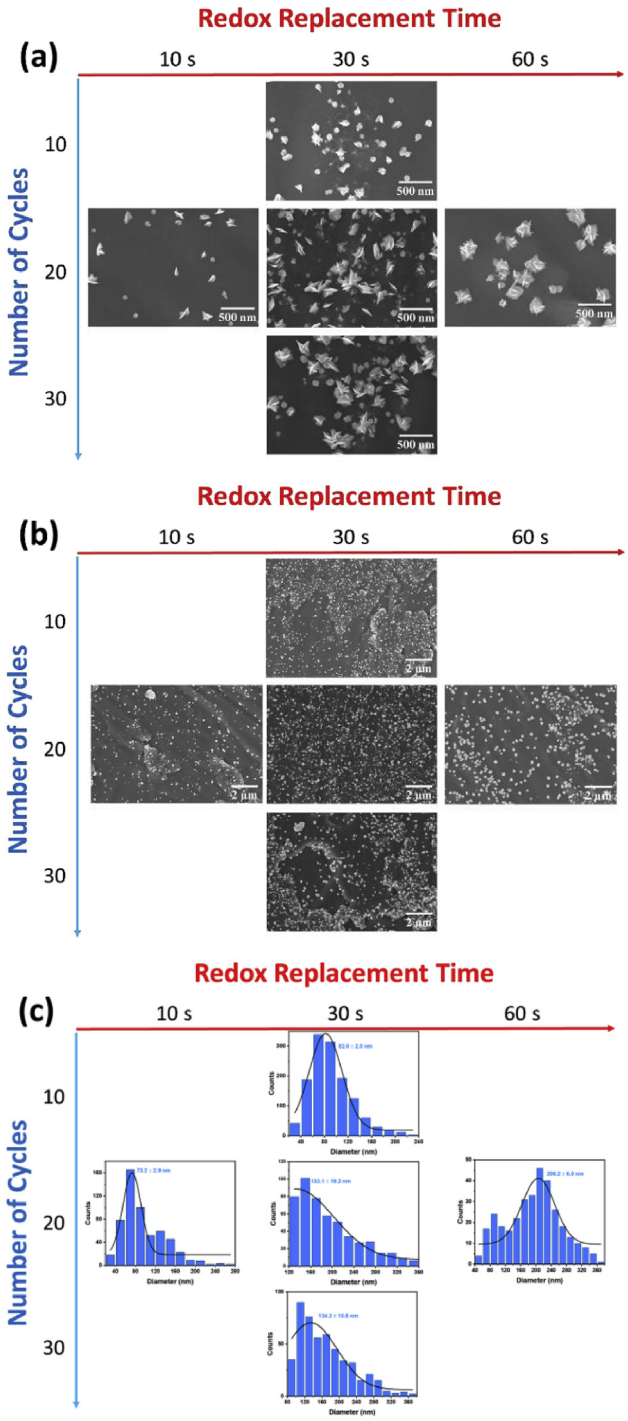

Fig. 5. Pt/Ni nanoparticles on flat TiO_2 surface prepared by EDRR method from 100 ppm Pt, 60 g/l Ni and 10 g/l H_2SO_4 solution: (a) SEM images at 50,000 magnification, (b) SEM images at 10,000 magnification, (c) size distribution and average particle size determined from SEM micrographs.

deposited Ni with Pt, due to the difference in electrochemical oxidation/reduction potentials - Pt^{2+} oxidises the electrodeposited Ni to soluble Ni^{2+} while it itself is simultaneously reduced to Pt and deposited to the surface (see Reactions 1–2).

Fig. 3 highlights the need of redox replacement (RR) step in the nanoparticle formation. The galvanostatic pulsing (i.e. ED step) alone is not an effective method for the formation of Pt/Ni nanoparticles as is clearly observed when comparing SEM images of a Pt/

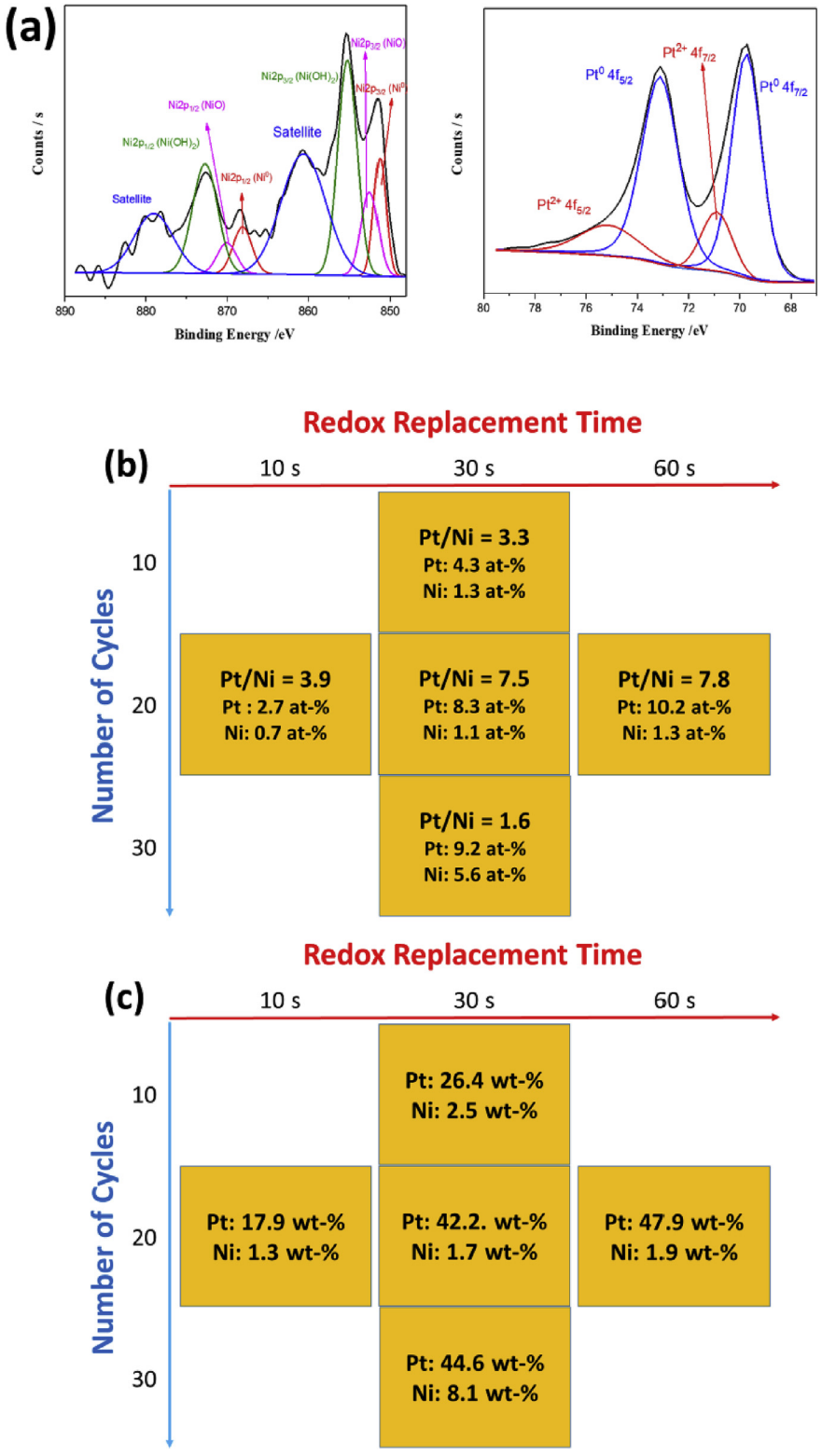

Fig. 6. (a) The XPS spectrum of Ni2p region (left) and Pt4f region (right), for a sample prepared on flat TiO_2 surfaces by EDRR method (redox replacement time: 30 s, number of cycles: 30) from 100 ppm Pt, 60 g/l Ni and 10 g/l H_2SO_4 solution, (b) the atomic-% and (c) weight-% of Pt and Ni on flat TiO_2 surface as a function of number of EDRR cycles and redox replacement time determined by XPS.

Ni nanoparticles prepared with galvanostatic pulsing to those prepared by EDRR method. The used parameters were the same in both of these cases, the only difference being that EDRR has an additional RR step/cycle. For comparison, Fig. 3 also shows the deposition of pure Ni nanoparticles by EDRR method and it is evident that although Pt is not necessary for the nucleation of particles on the surface, it improves it. In addition, the presence of Pt results in a characteristically jagged appearance of the nanoparticles (see Supporting Information, S2). This observation is probably a result of Pt growth on the nanoparticles, both during the redox replacement step and possible co-deposition on previously replaced Pt in the subsequent ED steps.

The positive effect of redox replacement step on nanoparticle formation is partly due to Ostwald ripening, leading to the presence of larger surface features, and partly due to the replenishing of solution nearby the electrode, reducing the possibility of mass-transfer limitation in ED step. Natter and Hempelmann (2003) have found a similar observation with pulse electrodeposition when varying t_{off} (i.e. short current-off time between deposition pulses) for Au nanoparticles, i.e. the size of nanoparticles grew with longer t_{off} time. It is important to note that - in addition to different materials and solutions (Au in literature (Natter and Hempelmann, 2003) *cf.* Pt/Ni presented here) - t_{off} time has a different purpose than RR time. In pulse electrodeposition, t_{off} is applied only for milliseconds between short deposition pulses and pulsing is performed in a single metal electrolyte in order to replenish the surface from adsorbed hydrogen, while RR time is clearly longer and performed after electrodeposition step in multi-metal electrolyte in order to redox replacement reaction to take place. As a result, enrichment of the more noble metal on the surface takes place.

The effect of the initial EDRR cycles on Pt/Ni nanoparticle nucleation is presented in Fig. 4, which comprises of Pt/Ni nanoparticles deposited to flat TiO_2 surface using a single cycle or 5 cycles (the redox replacement time: 30 s). As can be seen, already after a single EDRR cycle particles have nucleated on the surface, although the particle size is relatively small. When the number of cycles is increased, both the particle density and size of the particles increase substantially and start to show the characteristic jagged appearance. Data from XPS shows that the at-% of Pt is 0.29 after a single cycle and it increases to 5.77 at-% after 5 cycles, whereas of Ni at-% remains low (0.77% after 1 cycle *cf.* 0.87 at-% after 5 cycles), suggesting that even if Pt may co-deposit with Ni during electrodeposition step, it is deposited primarily during the redox replacement step.

The formation of Pt/Ni nanoparticles is further studied as a function of number of cycles and RR time (Fig. 5 – SEM and Fig. 6 - XPS). The associated potential profiles of EDRR (Fig. S1) are shown in Supporting Information.

From Fig. 5 it is seen that the size of nanoparticles increases both as a function of number of cycles and RR time. As previously discussed (Fig. 3), the positive effect of RR time on the size and nanoparticle density can be associated with Ostwald ripening and replenishing the solution nearby the electrode: the dissolution of Ni from the surface during RR step leads to a higher local concentration in the vicinity of the electrode, further diminishing the possible mass-transport limitation in the following ED step.

Fig. 6(a) shows examples of Ni2p and Pt4f spectra for a sample prepared from 100 ppm Pt solution on a TiO_2 surface using the EDRR method (the redox replacement time was 30 s and number of cycles 30). As can be seen, the Pt4f region has well separated spin-orbit components ($\Delta_{metal} = 3.35$eV).The atomic-% (and weight-%) of Pt was determined by considering the doublet peak of Pt4f region, which can be de-convoluted into four peaks. The presence of two main peaks (69.75 eV and 73.12 eV) is ascribed to the Pt^0 $4f_{7/2}$ and Pt^0 $4f_{5/2}$, while the other small peaks at 71.0 eV and 75.26 eV correspond to Pt^{2+} $4f_{7/2}$ and Pt^{2+} $4f_{5/2}$. Ni2p peak, on the other hand, has split spin-orbit components ($\Delta_{metal} = 17.3$eV) that comprise of core level and satellite features, which can be resolved into eight peaks. Two peaks are located at 851.25 eV (Ni^0 2p3/2) and 868.5 eV (Ni^0 2p1/2), indicating the presence of Ni metal. Another

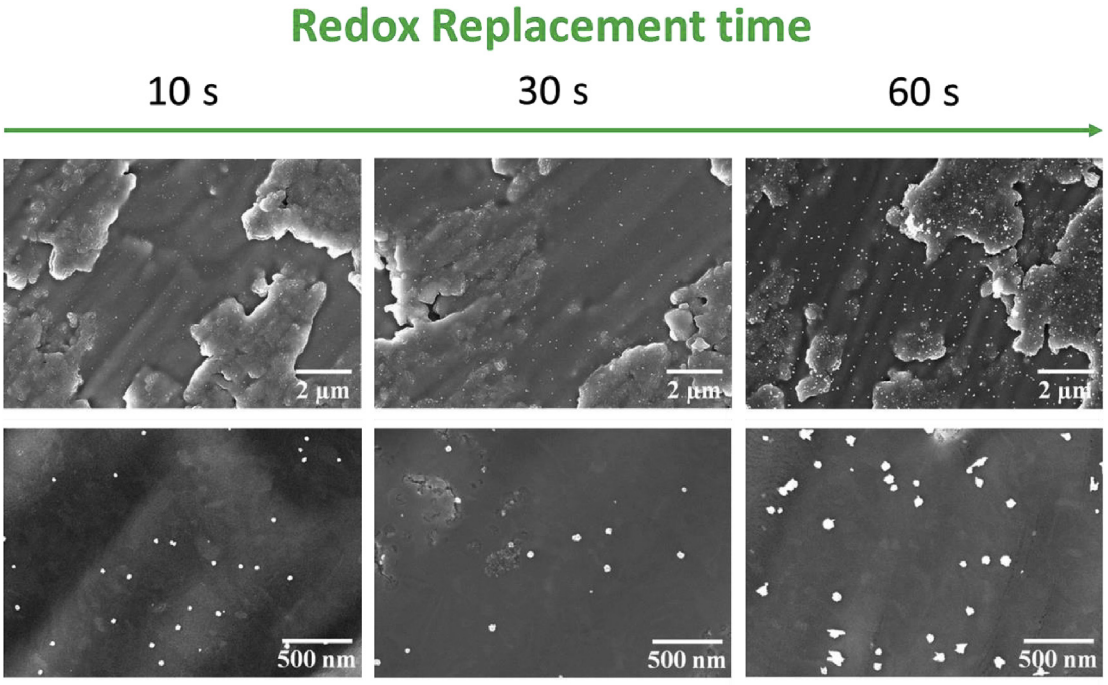

Fig. 7. Pt/Ni nanoparticles on flat TiO_2 surface prepared by EDRR method from 10 ppm Pt, 60 g/l Ni and 10 g/l H_2SO_4 solution. Number of cycles was 20 for each case; redox replacement time was varied. Upper row: magnification of 10,000, lower row: magnification of 50,000.

two peaks at 852.40 eV (Ni^{2+} 2p3/2) and 869.76 eV (Ni^{2+} 2p1/2) are ascribed to the NiO. The other two peaks at 855.14 eV (Ni^{2+} 2p3/2) and 872.44 eV (Ni^{2+} 2p1/2) are due to the formation of $Ni(OH)_2$. The peaks at 860.44 eV and 879.06 eV are the satellite peaks.

As can be observed from Fig. 6(b–c), also the atom-% of Pt (and the respective weight-% of Pt, both determined by XPS) increases with longer RR times. This is due to the mass-transfer limitations related to the low Pt concentration: the mass-transfer quickly limits the redox replacement reaction when Pt content is present only in ppm levels and thus, increasing the replacement time provides longer time for Pt to reach the electrode surface, resulting in higher Pt at-% on the surface. In order to demonstrate more clearly the purity of the end-product, the Pt/Ni ratio is calculated from at-% - Fig. 6(b) – and demonstrates that higher RR time results in higher end-product purity.

The effectiveness of the EDRR, on the other hand, is best discussed in terms of enrichment, which is calculated by comparing the weight-% of Pt on the particles (determined by XPS) to weight-% of Pt in the solution. It is remarkable how effective EDRR is when compared to pure galvanostatic pulsing (Figs. 3 and 6c). For example for a 100 ppm (1 ppm = 0.0001 wt-%) Pt solution, utilising 60 s RR time results in 42 weight-% of Pt on the surface after only 20 EDRR cycles, and this translates to over 4,200-fold enrichment. In comparison, the reference sample shown in Fig. 3 (30 cycles of galvanostatic pulsing and no RR steps) has a significantly lower Pt content (4.6 wt-%), resulting in a decade lower (460) enrichment, even if the current input in the reference sample is higher (20 cycles in EDRR *cf.* 30 cycles in galvanostatic pulsing).

To further demonstrate the industrial feasibility of the EDRR method, the formation of nanoparticles was performed from a solution containing only 10 ppm of Pt but with the same Ni concentration (60 g/l of Ni), resulting in concentration ratio Ni/Pt = 20,000. As can be seen in Fig. 7, the formation of Pt/Ni nanoparticles is successful even with such a low concentration of Pt in solution. Moreover, XPS analysis showed that with 60 s replacement time 15 wt-% of Pt was deposited on the surface, a level that is over three time higher than obtained by the pure galvanostatic pulsing (reference sample) from the 100 ppm Pt solution. In the terms of the enrichment, EDRR results in over 10,000-time enrichment of Pt from 10 ppm solutions, suggesting that the method is extremely feasible with the solutions with a low level of precious metals.

In order to investigate further the abilities of EDRR in the formation of the high-value added products, experiments were performed using TiO_2 nanotube substrates (Fig. 8 – SEM and Fig. 9 - XPS). TiO_2 nanotube surfaces are promising candidates for the photo-catalytic applications as the tubular configuration provides a high light absorption pathway and aids the prevention of the recombination of photo-generated electron/hole pairs (Tong et al., 2012). Moreover, TiO_2 nanotubes have demonstrated drastically enhanced photocatalytic activity in numerous studies when the nanotubes are decorated with “co-catalyst” metal nanoparticles (Christoforidis and Fornasiero, 2017; Liang et al., 2013; Ni et al., 2007; Papadimitriou et al., 2008; Park et al., 2013).

Figs. 8–9 demonstrate that the size and the amount of Pt/Ni nanoparticles on TiO_2 nanotube surface can indeed be controlled by RR time and cycling when using the EDRR method (see also Fig. S2b). The results also show that particles not only nucleate on the top of the nanotubes but also on the outer walls, allowing the exploitation of the 1D nature of the tubes for photocatalysis: the main advantages of 1D materials are the enhanced light absorption combined with short reaction paths of photogenerated carriers (Xiao et al., 2015; Altomare et al., 2016; Nguyen et al., 2015, 2016). Fig. 9(a) shows again an exemplar of the XPS data fitted for the Ni2p and Pt4f regions and the detected species were Pt^0, Pt^{2+} and Ni species. Furthermore, the EDRR method allows the control over the Pt/Ni ratio (Fig. 9(b), at-% determined by XPS) which has been shown to be a critically important factor in the electrocatalysis of oxygen reduction reaction in numerous studies (Jiang et al., 2017; Toda et al., 1999; Yang et al., 2004).

In order to demonstrate that the EDRR method could be used to produce photocatalytic surfaces from hydrometallurgical base metal streams, proof-of-concept measurements of photocatalytic H_2 generation with the prepared Pt/Ni nanoparticle - TiO_2 nanotube surfaces were performed. Fig. 10 shows that these surfaces indeed possess significant activity for H_2 evolution, the highest being an over 30-fold enhancement (the redox replacement step = 240 s and number of cycles = 20) when compared to a pure TiO_2 nanotube surface. When the photocatalytic activity is compared to TiO_2 nanotube surfaces covered with pure Ni nanoparticles, the H_2 evolution levels are similar for fresh samples (see Supporting Information, S3). However, pure Ni nanoparticles suffers from aging whereas Pt or Pt/Ni are highly stable against oxidation (S3). Moreover, the catalytic activity shown here is comparable with

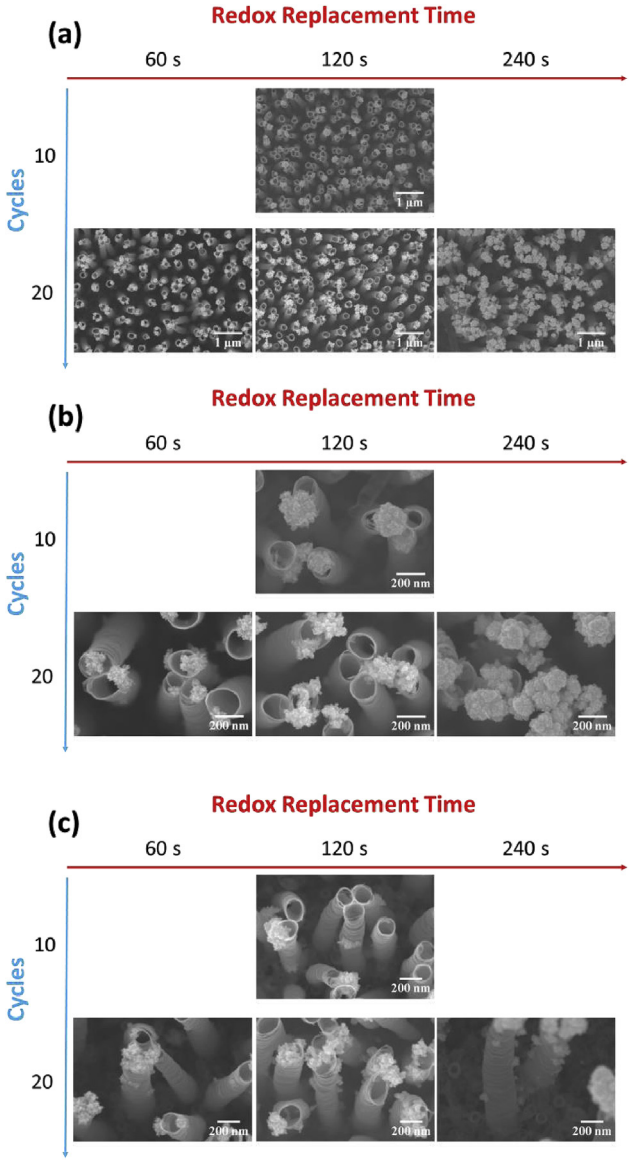

Fig. 8. Pt/Ni nanoparticles on TiO_2 nanotube surfaces prepared by EDRR from 100 ppm Pt, 60 g/l Ni and 10 g/l H_2SO_4 solution: SEM images at magnification of (a) 20,000, (b) 100,000 and (c) 80,000.

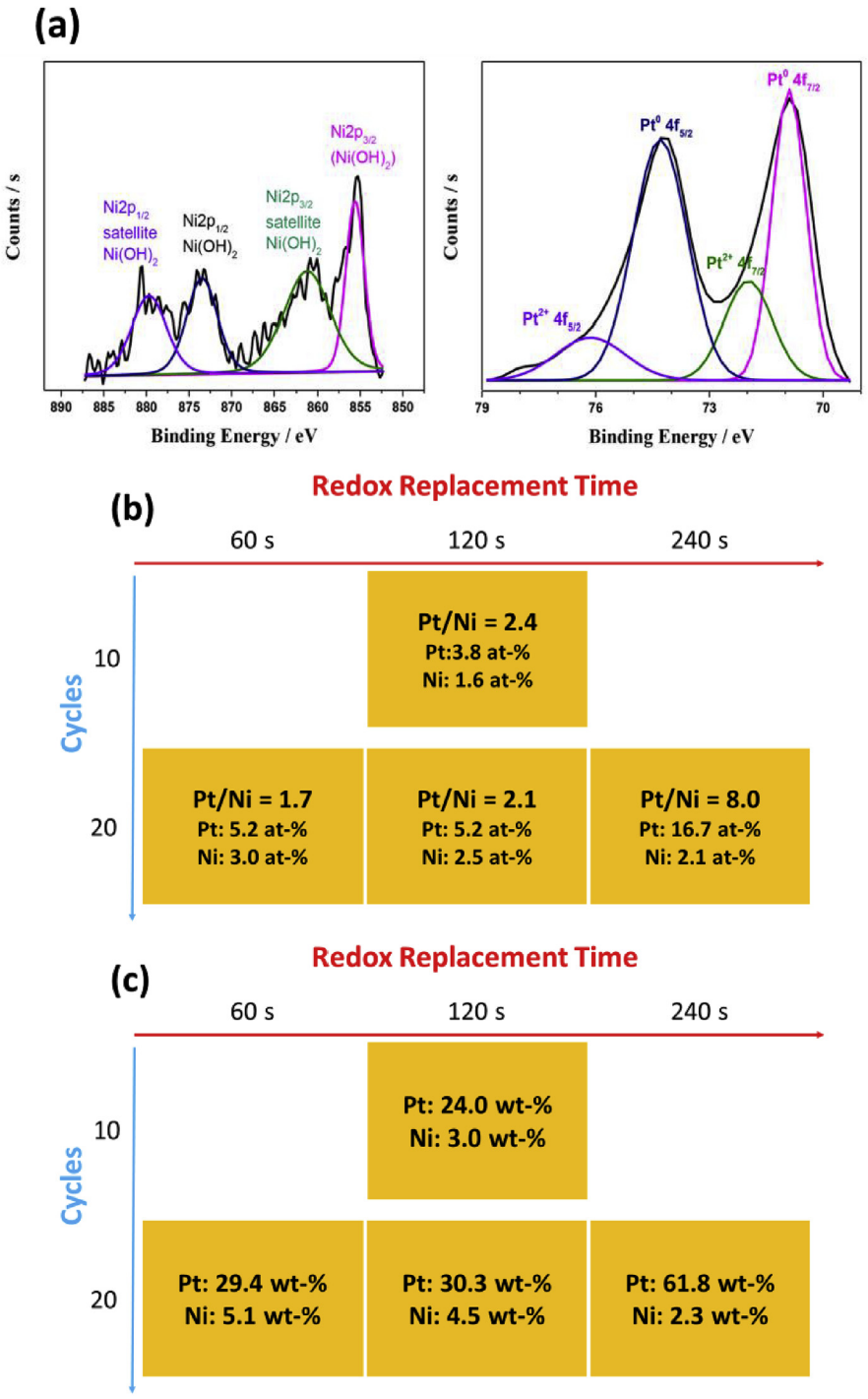

Fig. 9. (a) The XPS spectrum of Ni2p region (left) and Pt4f region (right), for a sample prepared on TiO_2 nanotube surfaces by EDRR method from 100 ppm Pt, 60 g/l Ni and 10 g/l H_2SO_4 solution (redox replacement time: 120 s, number of cycles: 20), (b) the atomic-% and (c) weight-% of Pt and Ni on TiO_2 nanotube surfaces as a function of number of cycles and redox replacement time, determined by XPS.

literature, e.g. our results show a similar H_2 evolution rate under 1.5 AM solar illumination as that obtained for atomic layer deposited Pt as co-catalysts on TiO_2 nanotubes (Yoo et al., 2018). The results also indicate that the Pt/Ni ratio is critical for H_2 evolution: the sample with highest H_2 production has also the clearly highest Pt/Ni ratio $\approx$ 8, while for all the other surfaces the Pt/Ni ratio $\approx$ 2 (Fig. 9(b)). All these samples with a similar Pt/Ni ratio have also similar hydrogen evolution rates (Fig. 10), thus indicating the critical role of Pt/Ni ratio in the particles.

As the presented EDRR method is particularly powerful in tuning the Pt/Ni composition, these results are very promising in the view of preparing photocatalytic surfaces directly from sulfate based process streams or side streams of hydrometallurgical Ni metal plants. EDRR is truly attractive approach for the industrial solutions that contain only a small amount of platinum group metals (PGMs), especially as Pt/Ni nanoparticle formation consumes electricity only during the Ni deposition steps while Pt is "enriched" on the surface via an electroless redox replacement

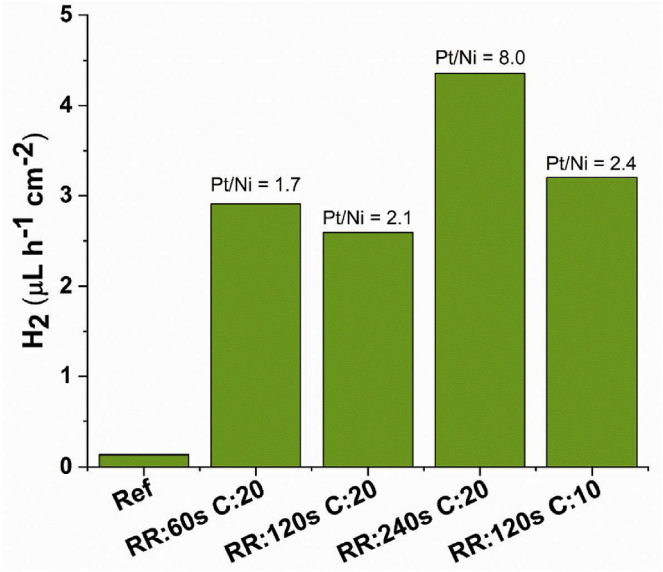

Fig. 10. Photocatalytic H_2 evolution by Pt/Ni nanoparticles on TiO_2 nanotube surface. Pt/Ni nanoparticles are deposited at different EDRR parameters (RR = redox replacement time, C = number of cycles). The reference sample (Ref) is pure TiO_2 nanotube surface.

reaction, thus enhancing the process economics. It is also worth noting that as EDRR was successful from solutions with Ni/Pt ratio as high as 20,000, the industrial Ni process solutions and side-streams containing trace amounts of PGMs could potentially be "a platinum mine" for clean energy technologies if a future industrial process was developed. For example, in an average size base metal plant 10 m^3/h or even 100 m^3/h of such solutions are flowing in the processes, and with such amounts the large-scale production of catalysts – which has been identified as one of the main task of catalyst development (Debe, 2012) - can truly become possible.

Real hydrometallurgical solutions also contain other metals than Ni and Pt and these will influence both the EDRR process and resultant surface. Previous results of Ag recovery from Zn/Ag solutions [Yliniemi et al., 2018] have shown that although the presence of Fe^{3+} as in impurity may slightly reduce enrichment efficiency, it may improve product purity. This is most likely due to the selective dissolution of Zn by Fe^{3+} as the reduction potential of Fe^{3+}/Fe^{2+} ($E^\circ = 0.77$ V vs. SHE) is higher than that of Zn^{2+}/Zn. Thus, both Fe^{3+} and Ag^+ can oxidise Zn to Zn^{2+} but only Ag is enriched on the surface as Fe^{3+} is reduced to soluble Fe^{2+}. Similar behaviour is expected in Ni/Pt solution and when considering performance, this may actually result in increased catalytic activity. Therefore, EDRR performed in hydrometallurgical solutions has huge potential for the recovery of precious metals like Ag (Halli et al., 2017; Yliniemi et al., 2018) and Au (Korolev et al., 2018). Furthermore, this paper shows that EDRR can also directly produce functionalised surfaces with Pt or other trace metals present in hydrometallurgical solutions. Moreover, EDRR method allows control over not only particle size and density, but more importantly, over the precious metal/base metal ratio (here Pt/Ni) in the particles, i.e. EDRR provides also a control over the catalytic activity of these surfaces.

4. Conclusions

The EDRR process outlined here is an effective method for the production of catalytic surfaces and simultaneously, exploiting the hydrometallurgical solutions fully by utilising also the minor components (such as Pt) present in them. Remarkably, the results presented here show a 10,000-time enrichment level of Pt onto the surface when Pt/Ni nanocatalysts are formed from solution simulating hydrometallurgical process streams on TiO_2 surfaces by EDRR. It is also noteworthy, that such an enrichment is possible without any additional use of chemical or further modifications.

By adjusting the different EDRR parameters (number of cycles or redox replacement time), the surface characteristics of the resultant catalytic nanoparticles can be tuned to control the desirable properties like nanoparticle size and distribution. Moreover, preliminary results of the produced Pt/Ni co-catalytic surfaces for photocatalytic H_2 evolution demonstrated the level of performance that is comparable to the standard procedures for co-catalytic Pt/TiO_2 surfaces found in literature.

Overall, the findings offer a more sustainable circular economy platform, where minor concentrations of valuable metals present in base metal production solutions are used for the preparation of high-value products to be used as photocatalysts in clean energy sector.

Acknowledgements

Academy of Finland (NoWASTE - project no: 297962), Finland; Technology Industries of Finland Centennial/Jane and Aatos Erkko Foundation (Future Makers: Biorefinery Side Stream Materials for Advanced Biopolymer Materials - BioPolyMet), Finland; ERC, European Union; DFG (the Erlangen DFG cluster of excellence EAM, project EXC 315 (Bridge) and funCOS), Germany.

Appendix A. Supplementary data

Supplementary data related to this article can be found at https://doi.org/10.1016/j.jclepro.2018.08.022.

References

Altomare, M., Nguyen, N.T., Schmuki, P., 2016. Templated dewetting: designing entirely self-organized platforms for photocatalysis. Chem. Sci. 7, 6865–6886.
Brankovic, S.R., Wang, J.X., Adžić, R.R., 2001. Metal monolayer deposition by replacement of metal adlayers on electrode surfaces. Surf. Sci. 474, L173–L179.
Christoforidis, K.C., Fornasiero, P., 2017. Photocatalytic hydrogen production: a rift into the future energy supply. ChemCatChem 9, 1523–1544.
Crundwell, F., Moats, M., Ramachandran, V., Robinson, T., Davenport, W.G., 2011. Extractive Metallurgy of Nickel, Cobalt and Platinum-group Metals, first ed. Elsevier, Amsterdam.
Debe, M.K., 2012. Electrocatalyst approaches and challenges for automotive fuel cells. Nature 486, 43–51.
Elshkaki, A., Reck, B.K., Graedel, T.E., 2017. Anthropogenic nickel supply, demand, and associated energy and water use. Resour. Conserv. Recycl. 125, 300–307.
Gregory, B.W., Stickney, J.L., 1991. Electrochemical atomic layer epitaxy (ECALE). J. Electroanal. Chem. 300, 543–561.
Halli, P., Elomaa, H., Wilson, B.P., Yliniemi, K., Lundström, M., 2017. Improved metal circular economy-selective recovery of minor Ag concentrations from Zn process solutions. ACS Sustain. Chem. Eng. 5, 10996–11005.
He, H., Xiao, P., Zhou, M., Zhang, Y., Jia, Y., Yu, S., 2011. Preparation of well-distributed Pt–Ni nanoparticles on/into TiO_2NTs by pulse electrodeposition for methanol photoelectro-oxidation. Catal. Commun. 16, 140–143.
He, H., Xiao, P., Zhou, M., Liu, F., Yu, S., Qiao, L., Zhang, Y., 2013. PtNi alloy nanoparticles supported on carbon-doped TiO_2 nanotube arrays for photo-assisted methanol oxidation. Electrochim. Acta 88, 782–789.
Jiang, K., Shao, Q., Zhao, D., Bu, L., Guo, J., Huang, X., 2017. Phase and composition tuning of 1D platinum-nickel nanostructures for highly efficient electrocatalysis. Adv. Funct. Mater. 1700830–1700836.
Kollia, C., Spyrellis, N., Amblard, J., Froment, M., Maurin, G., 1990. Nickel plating by pulse electrolysis: textural and microstructural modifications due to adsorption/desorption phenomena. J. Appl. Electrochem. 20, 1025–1032.
Korolev, I., Altinkaya, P., Halli, P., Hannula, P., Yliniemi, K., Lundström, M., 2018. Electrochemical recovery of minor concentrations of gold from cyanide-free cupric chloride leaching solutions. J. Clean. Prod. 186, 840–850.
Kühl, S., Strasser, P., 2016. Oxygen electrocatalysis on dealloyed Pt nanocatalysts. Top. Catal. 59, 1628–1637.
Liang, F., Zhang, J., Zheng, L., Tsang, C.-K., 2013. Selective electrodeposition of Ni into the intertubular voids of anodic TiO_2 nanotubes for improved photocatalytic properties. J. Mater. Res. 28, 405–410.
McDonald, R.G., Whittington, B.I., 2008a. Atmospheric acid leaching of nickel

laterites review Part I. Sulphuric acid technologies. Hydrometallurgy 91, 35–55.
McDonald, R.G., Whittington, B.I., 2008b. Atmospheric acid leaching of nickel laterites review Part II. Chloride and bio-technologies. Hydrometallurgy 91, 56–69.
Natter, H., Hempelmann, R., 2003. Tailor-made nanomaterials designed by electrochemical methods. Electrochim. Acta 49, 51–61.
Ni, M., Leung, M.K.H., Leung, D.Y.C., Sumathy, K., 2007. Review and recent developments in photocatalytic water-splitting using TiO_2 for hydrogen production. Renew. Sustain. Energy Rev. 11, 401–425.
Nguyen, N.T., Altomare, M., Yoo, J., Schmuki, P., 2015. Efficient photocatalytic H2 evolution: controlled dewetting-dealloying to fabricate site-selective high-activity nanoporous Au particles on highly ordered TiO_2 nanotube arrays. Adv. Mater. 27, 3208–3215.
Nguyen, N.T., Altomare, M., Yoo, J.E., Taccardi, N., Schmuki, P., 2016. Noble metals on anodic TiO2 nanotube mouths: thermal dewetting of minimal Pt co-catalyst loading leads to significantly enhanced photocatalytic H2 generation. Adv. Energy Mater. 6, 1501926.
Papadimitriou, S., Armyanov, S., Valova, E., Hubin, A., Steenhaut, O., Pavlidou, E., Kokkinidis, G., Sotiropoulos, S., 2010. Methanol oxidation at Pt-Cu, Pt-Ni, and Pt-Co electrode coatings prepared by a galvanic replacement process. J. Phys. Chem. C 114, 5217–5223.
Papadimitriou, S., Tegou, A., Pavlidou, E., Armyanov, S., Valova, E., Kokkinidis, G., Sotiropoulos, S., 2008. Preparation and characterisation of platinum- and gold-coated copper, iron, cobalt and nickel deposits on glassy carbon substrates. Electrochim. Acta 53, 6559–6567.
Park, H., Park, Y., Kim, W., Choi, W., 2013. Surface modification of TiO_2 photocatalyst for environmental applications. J. Photochem. Photobiol. C Photochem. Rev. 15, 1–20.
Peck, D., Kandachar, P., Tempelman, E., 2015. Critical materials from a product design perspective. Mater. Des. 65, 147–159.
Rettew, R.E., Guthrie, J.W., Jaye, C., Fischer, D., Alamgir, F.M., 2009. Synthesis and characterization of monolayer bimetallic surfaces: a synchrotron. ECS Trans. 19, 97–106.
Shao, M., Chang, Q., Dodelet, J.-P., Chenitz, R., 2016. Recent advances in electrocatalysts for oxygen reduction reaction. Chem. Rev. 116, 3594–3657.
Spanou, S., Pavlatou, E.A., 2010. Pulse electrodeposition of Ni/nano-TiO_2 composites: effect of pulse frequency on deposits properties. J. Appl. Electrochem. 40, 1325–1336.
Tamašauskaitė-Tamašiūnaitė, L., Balčiūnaitė, A., Zabielaitė, A., Vaičiūnienė, J., Selskis, A., Pakštas, V., Norkus, E., 2013. Investigation of electrocatalytic activity of titania nanotube supported nanostructured PteNi catalyst towards methanol oxidation. J. Electroanal. Chem. 707, 31–37.
Tamašauskaitė-Tamašiūnaitė, L., Balčiūnaitė, A., Zabielaitė, A., Vaičiūnienė, J., Juškėnas, R., Selskis, A., Norkus, E., 2014. Ethanol electro-oxidation in an alkaline medium using the nanostructured platinum-nickel electrocatalysts. ECS Trans. 59, 247–257.
Tegou, A., Papadimitriou, S., Kokkinidis, G., Sotiropoulos, S., 2010. A rotating disc electrode study of oxygen reduction at platinised nickel and cobalt coatings. J. Solid State Electrochem. 14, 175–184.
Toda, T., Igarashi, H., Uchida, H., Watanabe, M., 1999. Enhancement of the electroreduction of oxygen on Pt alloys with Fe, Ni, and Co. J. Electrochem. Soc. 146, 3750–3756.
Tong, H., Ouyang, S., Bi, Y., Umezawa, N., Oshikiri, M., Ye, J., 2012. Nano-photocatalytic materials: possibilities and challenges. Adv. Mater. 24, 229–251.
Vaidyanathan, R., Cox, S.M., Happek, U., Banga, D., Mathe, M.K., Stickney, J.L., 2006. Preliminary studies in the electrodeposition of PbSe/PbTe superlattice thin films via electrochemical atomic layer deposition (ALD). Langmuir 22, 10590–10595.
Wang, J.X., Ma, C., Choi, Y.-M., Su, D., Zhu, Y., Liu, P., Si, R., Vukmirovic, M.B., Zhang, Y., Adžić, R.R., 2011. Kirkendall effect and lattice contraction in nanocatalysts: a new strategy to enhance sustainable activity. J. Am. Chem. Soc. 133, 13551–13557.
Xiao, F.-X., Miao, J., Tao, H.B., Hung, S.-F., Wang, H.-Y., Yang, H.B., Chen, J., Chen, R., Liu, B., 2015. One-dimensional hybrid nanostructures for heterogeneous photocatalysis and photoelectrocatalysis. Small 11, 2115–2131.
Yang, H., Vogel, W., Lamy, C., Alonso-Vante, N., 2004. Structure and electrocatalytic activity of carbon-supported Pt-Ni alloy nanoparticles toward the oxygen reduction reaction. J. Phys. Chem. B 108, 11024–11034.
Yliniemi, K., Wang, Z., Korolev, I., Hannula, P., Halli, P., Lundström, M., 2018. Effect of impurities in precious metal recovery by electrodeposition-redox replacement method from industrial side-streams and process streams. ECS Trans. 85, 59–67.
Yoo, J., Zazpe, R., Cha, G., Prikryl, J., Hwang, I., Macak, J.M., Schmuki, P., 2018. Uniform ALD deposition of Pt nanoparticles within 1D anodic TiO_2 nanotubes for photocatalytic H_2 generation. Electrochem. Commun. 86, 6–11.
Zhang, C., Yu, H., Li, Y., Song, W., Yi, B., Shao, Z., 2012. Preparation of Pt catalysts decorated TiO_2 nanotube arrays by redox replacement of Ni precursors for proton exchange membrane fuel cells. Electrochim. Acta 80, 1–6.